

6-(Arylvinylen)-3-bromopyridine Derivatives as Lego Building Blocks for Liquid Crystal, Nonlinear Optical, and Blue Light Emitting Chromophores

Nicolas Leclerc,[†] Sébastien Sanaur,[‡] Laurent Galmiche,[†] Fabrice Mathevet,[†] André-Jean Attias,^{*,†,‡} Jean-Louis Fave,[§] Joseph Roussel,[§] Philippe Hapiot,^{||} Noëlla Lemaître,[⊥] and Bernard Geffroy[⊥]

Université Pierre et Marie Curie, UMR CNRS 7610, Chimie des Polymères, 4, place Jussieu, Case Courrier 185, F 75252, Paris Cedex 05, France, ONERA, Département des Matériaux et Systèmes Composites, 29, avenue de la Division Leclerc, B. P. 72, F 92322, Châtillon Cedex, France, GPS, Université Pierre et Marie Curie, UMR CNRS 75-88, 4, place Jussieu, F 75252, Paris Cedex 05, France, Université de Rennes 1, UMR 6510, Laboratoire d'Electrochimie Moléculaire et Macromoléculaire Synthèse et Electrosynthèse Organiques, Campus de Beaulieu, Bat. 10C, F 35042 Rennes Cedex, France, and CEA Saclay, DRT/LITEN/DSEN/GENEC/L2C, F 91191, Gif-sur-Yvette Cedex, France

Received July 20, 2004. Revised Manuscript Received November 2, 2004

A novel general synthetic strategy, based on a convergent approach, allowed us to prepare a series of conjugated 6,6'-distyryl-3,3'-bipyridine derivatives via the Suzuki reaction. First, the key electron-donor and electron-acceptor 6-(arylvinylen)-3-bromopyridine building blocks were synthesized by Knoevenagel- or Siegrist-type reactions. Second, some of them were transformed to the corresponding pyridylboronic esters. Finally, for the first time, we successfully demonstrated that such blocks can be homo- and cross-coupled in high yields and multigram scales, leading to noncentrosymmetric or symmetric chromophores. Their mesogenic, electrochemical, and optical properties have been investigated depending on the electronic structure. In this series, push–pull compounds are liquid crystals and promising for NLO applications. Whatever the structure, all of these compounds exhibit a high electron affinity and are strongly fluorescent. As an application, lasing properties of one push–pull and one symmetrical compound are reported. In addition, a blue-emitting LED was fabricated whose performances at 10 mA/cm² are a luminous efficiency of 3.9 cd/A, a power efficiency of 1.4 lm/W, and an external quantum efficiency of 2.9%. Thus, this versatile synthetic route is of particular interest due to the potential applications of the chromophores in several optoelectronic fields.

1. Introduction

π -Conjugated organic compounds have emerged in the past two decades as a promising class of materials for potential applications in photonics and optoelectronics. The active materials used in these fields are mainly polymers. Besides fully conjugated main-chain polymers used in third-order nonlinear optics (NLO),^{1,2} photovoltaic cells,³ light emitting devices (LEDs),⁴ and optically pumped lasers^{5a,b} are the partially conjugated alternating main-chain copolymers

(*alt*MCPs) and the side-chain polymers (SCPs) that have been investigated as active layers in LEDs,⁶ as solid-state lasers,^{5c} and mainly as second-order NLO materials in electrooptic (EO) devices.^{1,7} In these *alt*MCPs and SCPs, well-defined active conjugated chromophores are covalently bounded

* Corresponding author. Tel: (+33) 1 44 27 53 02. Fax: (+33) 1 44 27 70 89. E-mail: attias@ccr.jussieu.fr.

[†] Université Pierre et Marie Curie.

[‡] ONERA.

[§] GPS, Université Pierre et Marie Curie.

^{||} Université de Rennes 1.

[⊥] CEA Saclay.

- (1) Nalwa, H. S.; Miyata, S. *Nonlinear Optics of Organic Molecules and Polymers*; CRC Press: Boca Raton, FL, 1997.
- (2) Gubler, U.; Bosshard, C. *Adv. Polym. Sci.* **2001**, *158*, 123–191.
- (3) (a) Sariciftci, N. S.; Smilowitz, L.; Heeger, A. J.; Wudl, F. *Science* **1992**, *258*, 1474–1476. (b) Halls, J. J. M.; Walsh, C. A.; Greenham, N. C.; Marseglia, E. A.; Friend, R. H.; Moratti, S. C.; Holmes, A. B. *Nature* **1995**, *376*, 498–500. (c) Brabec, C. J.; Sariciftci, N. S.; Hummelen, J. C. *Adv. Funct. Mater.* **2001**, *11*, 15–26.
- (4) (a) Burroughes, J. H.; Bradley, D. D. C.; Brown, A. R.; Marks, R. N.; Mackay, K.; Friend, R. H.; Burns, P. L.; Holmes, A. B. *Nature* **1990**, *347*, 539–541. (b) Kraf, A.; Grimsdale, A. C.; Holmes, A. B. *Angew. Chem., Int. Ed.* **1998**, *37*, 402–428.

- (5) (a) Hide, F.; Diaz-Garcia, M.; Schwartz, B.; Andersson, M.; Pei, Q.; Heeger, A. J. *Science* **1996**, *273*, 1833. (b) Tessler, N.; Denton, G. J.; Friend, R. H. *Nature* **1996**, *382*, 695. (c) Costela, A.; Garcia-Moreno, I.; Figuera, J. M.; Amat-Guerri, F.; Sastre, R. *Appl. Phys. Lett.* **1996**, *68*, 593.
- (6) (a) Baigent, D. R.; Friend, R. H.; Lee, J. K.; Schrock, R. R. *Synth. Met.* **1995**, *71*, 2171–2172. (b) Boyd, T. J.; Geerts, Y.; Lee, J.-K.; Fogg, D. E.; Lavoie, G. G.; Schrock, R. R.; Rubner, M. F. *Macromolecules* **1997**, *30*, 3553–3559. (c) Bao, Z.; Peng, Z.; Galvin, M. E.; Chandross, E. A. *Chem. Mater.* **1998**, *10*, 1201–1204. (d) Shim, H.-K.; Jin, J.-I. *Adv. Polym. Sci.* **2001**, *158*, 193. (e) Bouché, C. M.; Berdagué, P.; Facoetti, H.; Robin, P.; Le Barny, P.; Schott, M. *Synth. Met.* **1996**, *81*, 191–195. (f) Yang, Z.; Hu, B.; Karasz, F. E. *J. Macromol. Sci., Pure Appl. Chem.* **1998**, *A35*, 233. (g) Beaupré, S.; Ranger, M.; Leclerc, M. *Macromol. Rapid Commun.* **2000**, *21*, 1013.
- (7) (a) Dalton, L. *Adv. Polym. Sci.* **2001**, *158*, 1–121. (b) Wu, X.; Wu, J.; Liu, Y.; Jen, A. K.-Y. *J. Am. Chem. Soc.* **1999**, *121*, 472. (c) Wang, F.; Ren, A. S.; He, M.; Harper, A. W.; Dalton, L. R.; Garner, S. M.; Zang, H.; Chen, A.; Steier, W. H. *Polym. Mater. Sci. Eng.* **1998**, *78*, 42. (d) Zhang, C.; Wang, C.; Dalton, L. R.; Zhang, H.; Steier, W. H. *Macromolecules* **2001**, *34*, 253. (e) He, M. Q.; Leslie, T. M.; Sinicropi, J. A. *Chem. Mater.* **2002**, *14*, 4662. (f) He, M. Q.; Leslie, T. M.; Sinicropi, J. A.; Garner, S. M.; Reed, L. D. *Chem. Mater.* **2002**, *14*, 4669. (g) Liu, S.; Haller, M. A.; Ma, H.; Dalton, L. R.; Jang, S. H.; Jen, K.-Y. *Adv. Mater.* **2003**, *15*, 603.

along the main chain or as pendant groups on a saturated polymer backbone, respectively. Thus, whatever the application, a first key requirement imposed on the design of such chromophores involves that they contain at least one end-capped functional group. The other requirements depend on the application. In the field of the LEDs, although various kinds of organic fluorescent dyes have been developed to obtain all three primary colors, there is a major challenge in the design of efficient blue light emitting chromophores, on one hand, and with the electron injection ability on the other hand.^{4b} To succeed, it is essential to adjust the highest occupied and the lowest unoccupied molecular orbitals (HOMO and LUMO energy levels, respectively) of the emitting molecule. In addition, if there are no rules concerning the symmetry of photoluminescent dyes, this is not the case for NLO chromophores. Indeed, on one hand, it has been found recently that symmetrical conjugated molecules with donor–acceptor–donor (D–A–D) and acceptor–donor–acceptor (A–D–A) structural motifs exhibit large third-order nonlinear properties (two-photon absorption, Kerr effect).^{8,9} On the other hand, it is well known that the second-order NLO properties (molecular hyperpolarizability (β)) arise from a noncentrosymmetric π -conjugated charge-transfer molecule containing both electron-acceptor and electron-donor groups connected by an electron-transmitting bridge (push–pull structure, characterized by a large dipole moment, μ).^{1,10} The NLO polymeric materials incorporating these chromophores are poled with an electric field to achieve a noncentrosymmetric dipole alignment at the macroscopic level. Recently, remarkable progress was made in the design and synthesis of chromophores with exceptionally high $\mu\beta$ values, up to $18\,000 \times 10^{-48}$ esu at $1.9\ \mu\text{m}$.⁷ Unfortunately, the bulk nonlinearity of the polymers decays rapidly, due to the relaxation of dipolar alignment.^{7a} An attractive alternative to these typical side-chain polymers is side-chain liquid crystal polymers (SCLCPs) in which the NLO chromophores possess mesogenic properties.¹¹ Indeed, liquid crystals have directional order that allows enhanced field-induced polar order.

In previous papers,^{12,13} we described a novel class of conjugated chromophores based on a 3,3'-bipyridine core. High electron affinity and mesogenic properties are expected

from the electron deficiency of the pyridinic ring and the planarity of the 3,3'-bipyridine core, respectively. Thus, symmetrical and push–pull chromophores were prepared via, respectively, a single or a double Knoevenagel-type condensation, under acidic conditions, of 6,6'-dimethyl-3,3'-bipyridine derivatives with corresponding aromatic aldehydes: thienyl ring as the donor group, or benzene ring *para*-substituted with electron-donor (D) or electron-acceptor (A) groups. By lateral substitutions of the π -conjugated bridge and by varying the nature of the acceptor/donor pair, we were able to tune the mesogenic,^{12,13} electrochemical,^{12,13} photoluminescent,^{12,13} and second- as well as third-order NLO properties of the chromophores.^{9,13} It should be noted that none of these chromophores were end-capped by a functional group. Thus, considering all of the above molecules as model compounds, the use of aldehydes bearing reactive functional groups (e.g., hydroxyl groups) should offer the opportunity to synthesize reactive chromophores able to be incorporated into a macromolecular chain, to obtain polymers exhibiting NLO and/or emitting properties. However, despite the above-mentioned attractive features, the previous two steps' synthetic route, in the case of the nonsymmetric chromophores, restricts the yield because of separation and purification difficulties, and consequently the potential combinations of donor/acceptor pairs. This is the reason it was necessary to define a new more efficient and general synthetic route to obtain unsymmetrical as well as symmetrical chromophores end-capped with reactive functional group(s) (e.g., hydroxyl groups) to covalently incorporate them into a polymer.

While synthetic approaches to 2,2'-bipyridines and its derivatives are well-established in the literature, there are few strategies leading to unsymmetrical disubstituted 2,2'-bipyridines. Concerning substituted 3,3'-bipyridines, few general routes have been described whatever the symmetry of the molecule: besides the synthesis of symmetrical 6,6'-disubstituted-3,3'-bipyridines by a Ni(0)-coupling of 3-halopyridines,¹⁴ only, to our knowledge, the synthesis of 3-heteroarylpyridines,¹⁵ and unsubstituted symmetric 3,3'-bipyridines,¹⁶ by Pd(0)-catalyzed cross-coupling of 3-stannylpyridines or 3-pyridylboranes with heteroaryl halides or 3-bromopyridine, respectively, have been reported in the literature.¹⁷ In this context, it was a challenge to define a new, versatile, and more efficient synthetic route, which allows the preparation of unsymmetrical π -conjugated 6,6'-disubstituted-3,3'-bipyridine derivatives. We recently de-

- (8) Albota, M.; Beljonne, D.; Brédas, J.-L.; Ehrlich, J. E.; Fu, J.-Y.; Heikal, A. A.; Hess, S. E.; Kogej, T.; Levin, M. D.; Marder, S. R.; McCord-Maughon, D.; Perry, J. W.; Röckel, H.; Rumi, M.; Subramaniam, G.; Webb, W.; Wu, X.-L.; Xu, C. *Science* **1998**, *281*, 1653–1656.
- (9) Chéroux, F.; Attias, A.-J.; Maillotte, H. *Adv. Funct. Mater.* **2002**, *12*, 203–208.
- (10) (a) Alheim, M.; Barzoukas, M.; Bedworth, P. V.; Blanchard-Desce, M.; Fort, A.; Hu, Z. Y.; Marder, S. R.; Perry, J. W.; Runser, C.; Staehelin, M.; Zysset, B. *Science* **1996**, *271*, 335–337. (b) Marder, S. R.; Kippelen, B.; Jen, A. K.-Y.; Peyghambarian, N. *Nature* **1997**, *388*, 845. (c) Jen, A. J.-K.; Rao, V. P.; Wong, K. Y.; Drost, K. J. *J. Chem. Soc., Chem. Commun.* **1993**, 90. (d) Jen, A. K.-Y.; Cai, Y.; Bedworth, P. V.; Marder, S. R. *Adv. Mater.* **1997**, *9*, 132.
- (11) (a) Singer, K. D.; Kuzyk, M. G.; Sohn, J. E. *J. Opt. Soc. Am. B: Opt. Phys.* **1987**, *4*, 968. (b) Van der Vorst, C. P. J. M.; Picken, S. J. *Proc. SPIE* **1987**, 866, 99. (c) Van der Vorst, C. P. J. M.; Picken, S. J. *J. Opt. Soc. Am.* **1990**, *B7*, 320. (d) Gonin, D.; Noël, C.; Le Borgne, A.; Gadret, G.; Kajzar, F. *Makromol. Chem., Rapid Commun.* **1992**, *13*, 537. (e) Gonin, D.; Guichard, B.; Noël, C.; Kajzar, F. In *Polymers and Other Advanced Materials: Emerging Technologies and Business Opportunities*; Prasad, P. N., et al., Eds.; Plenum Press: New York, 1995; pp 465–483. (f) Dubois, J. C.; Le Barny, P.; Mauzac, M.; Noël, C. *Acta Polym.* **1997**, *48*, 47.
- (12) (a) Attias, A.-J.; Cavalli, C.; Bloch, B.; Guillou, N.; Noël, C. *Chem. Mater.* **1999**, *11*, 2057–2068. (b) Attias, A.-J.; Hapiot, P.; Wintgens, V.; Valat, P. *Chem. Mater.* **2000**, *12*, 461–471. (c) Lemaître, N.; Attias, A.-J.; Ledoux, I.; Zyss, J. *Chem. Mater.* **2001**, *13*, 1420–1024.
- (13) (a) Chen, Q.; Sargent, E. H.; Leclerc, N.; Attias, A.-J. *Appl. Phys. Lett.* **2003**, *82*, 4420–4422. (b) Chen, Q.; Sargent, E. H.; Leclerc, N.; Attias, A.-J. *Appl. Opt.* **2003**, *42*, 7235–72241.
- (14) Constable, E. C.; Morris, D.; Carr, S. *New J. Chem.* **1998**, 287 and references therein.
- (15) (a) Ishikura, M.; Kamada, M.; Terashima, M. *Synthesis* **1984**, 936–938. (b) Gronowitz, S.; Björk, P.; Malm, J.; Hörnfeld, A.-B. *J. Org. Chem.* **1993**, *58*, 127–129. (c) Bouillon, A.; Lancelot, J. C.; Collot, V.; Bovy, P. R.; Rault, S. *Tetrahedron* **2002**, *58*, 3323–3328.
- (16) (a) Lopez, S.; Kahraman, M.; Harmata, M.; Keller, S. W. *Inorg. Chem.* **1997**, *36*, 6138–6140. (b) Radig, R. S.; Lam, R.; Zavalij, O. Y.; Katala Ngala, J.; LaDuca, R. L.; Greedam, J. E.; Zubietta, J. *Inorg. Chem.* **2002**, *41*, 2124–2133.
- (17) Linda, P.; Marino, G.; Santini, S. *Tetrahedron Lett.* **1970**, *11*, 4223–4224.

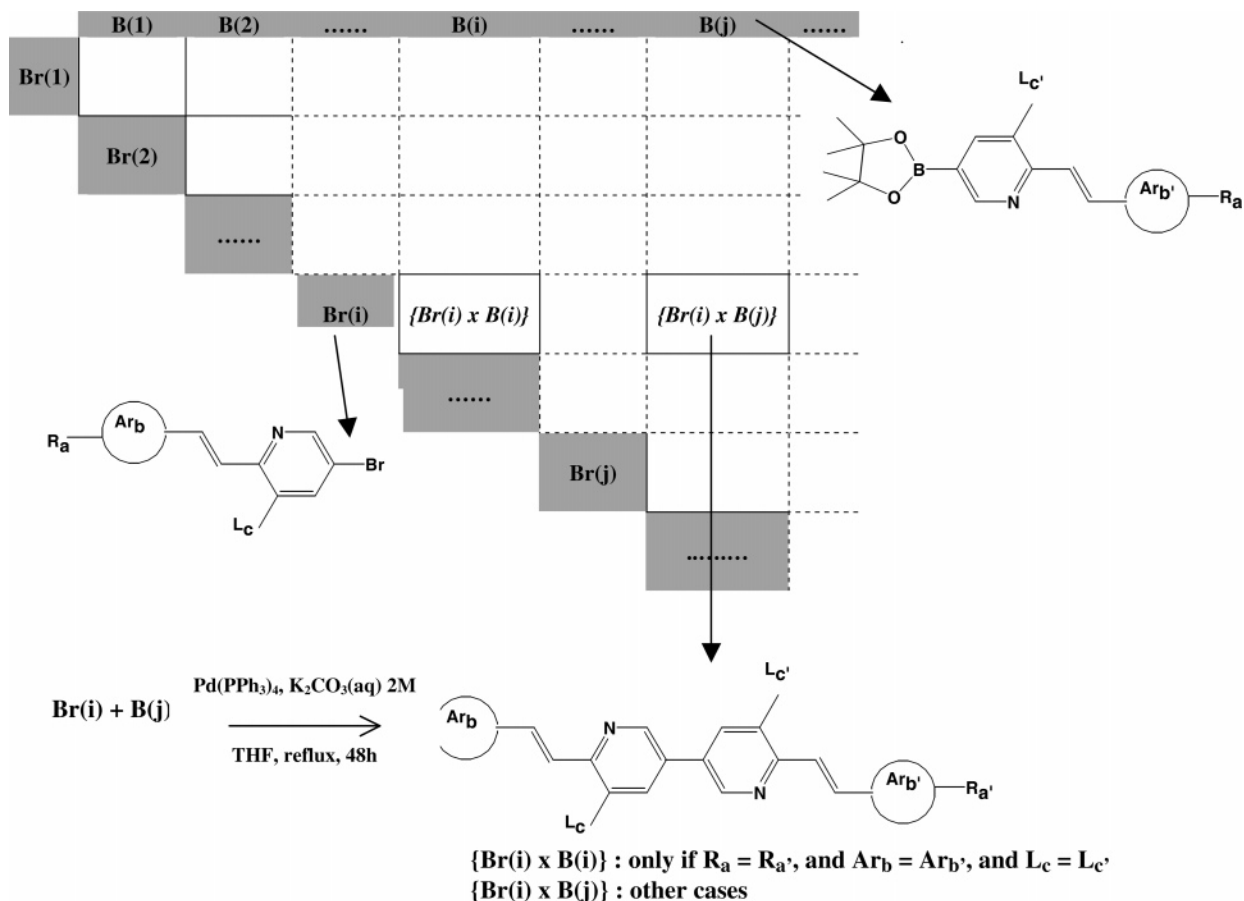


Figure 1. Schematic representation of the convergent synthetic route.

scribed a new general route to access to 6,6'-(disubstituted)-3,3'-bipyridine-based chromophores.¹⁸ This new large-scale strategy is based, as described in Figure 1, on (i) the synthesis of a library of conjugated 6-substituted-3-bromopyridine building blocks (**Br(i)**; horizontal entry of the matrix), (ii) their transformation to 6-substituted-3-pyridylboronic ester building blocks (**B(i)**; vertical entry of the matrix), and (iii) the cross-coupling $\{\text{Br(i)} \times \text{B(j)}\}$ (off-diagonal terms of the matrix) by the metal-catalyzed Suzuki reaction. The main advantage of this synthetic pathway is the flexibility to combine “tailor-made” building blocks depending on the expected mesogenic, electrochemical, or optical properties of the chromophore. It should be noted that this route allows also the synthesis of symmetrical compounds ($\{\text{Br(i)} \times \text{B(i)}\}$; on-diagonal terms of the matrix).

The present contribution (i) describes in detail this more efficient and convenient strategy for the synthesis of the building blocks, by giving three alternative routes, among which is an adaptation of the Siegrist reaction, (ii) presents the mesogenic and optical properties of a novel push–pull chromophore, (iii) presents the preliminary results of the lasing properties of a blue-emitting chromophore, and (iv) presents the electroluminescent properties and the characteristics of a multilayer OLED incorporating this dye. The results demonstrate that this “combinatorial”-type synthetic route represents a versatile powerful strategy for developing

multifunctional chromophores. All of the compounds were characterized by means of ¹H and ¹³C NMR spectroscopies, differential scanning calorimetry (DSC), UV/visible, and fluorescence spectroscopies in solution. Polarized-light optical microscopy (POM), X-ray diffraction (XRD), and cyclic voltammetry were used for the mesogenic and electrochemical characterizations, respectively.

2. Experimental Section

2.1. Techniques. 2.1.1. Nuclear Magnetic Resonance (NMR) Spectroscopy. ¹H and ¹³C NMR spectra were recorded on a Brüker ARX 250 instrument. Chloroform-*d* (CDCl₃) or methyl sulfoxide-*d*₆ (DMSO-*d*₆) was used as the solvent.

2.1.2. Thermal Analysis. Melting points were measured on a TA Instruments DSC 2920-Modulated DSC operating at 5 °C/min under nitrogen.

2.1.3. Phase Behavior. Textures were observed on a Leitz Ortholux polarizing optical microscope equipped with a Mettler FP 82 heating stage attached with a Mettler FP 80 temperature controller.

2.1.4. X-ray Diffraction (XRD). The XRD patterns were obtained by filling the crude powder in Lindemann capillaries of 1 mm diameter. A linear monochromatic Cu Kα₁ beam ($\lambda = 1.5405$ Å) obtained with sealed-tube generator (900 W) and a bent quartz monochromator were used. The diffraction patterns were registered with a curved counter Inel CPS 120. In this setup, the exposure time was 1 h, every 10 °C; the sample temperature was controlled within ± 0.05 °C; periodicities up to 60 Å can be measured. The cell parameters were calculated from the position of the reflection at the smallest Bragg angle, which is in all cases the most intense.

(18) (a) Leclerc, N.; Serieys, I.; Attias, A.-J. *Tetrahedron Lett.* **2003**, *44*, 5879–5882. (b) Leclerc, N.; Galmiche, L.; Attias, A.-J. *Tetrahedron Lett.* **2003**, *44*, 5883–5887.

2.1.5. Optical Spectroscopies. The UV–visible absorbance spectra were recorded on a spectrometer Perkin-Elmer Lambda 18. A 1 cm quartz cell was used, and the concentrations were chosen so that the appropriate absorbance values (0.1–0.2) were obtained at λ_{max} . The emission spectra were obtained from the same solution, using an Aminco S.L.M. 8100 luminescence spectrometer.

2.1.6. Lasing Properties. Photoluminescence and laser emission spectra were measured using a Nd³⁺:YAG pumped dye-laser as the excitation source (3.5 eV, 355 nm). The excitation pulses had a temporal width of 10 ns, and pulses energies varied from 50 μ J to 2.9 mJ at 10 Hz repetition rate. Sample light emission was focused on the entrance slit of a TRIAX 190 (Jobin Yvon) spectrometer and was detected by a Photonis photomultiplier. Slit widths were 50 μ m (0.3 nm resolution). The circulating dye cell containing chromophores displayed in Figure 1S consists of a cylindrical tube finished by port-hole on extremities. The laser cavity was defined by an $R = 100\%$ mirror from 400 to 700 nm and a wedge as the output coupler. The pump light was focused onto the dye solution by a cylindrical lens ($f = 50$ mm), which created a narrow optically excited region across the curve. Photoluminescence spectra were performed in the same setup without mirror $R = 100\%$. All measurements were performed at room temperature under standard atmosphere. The solvent (1 L) was 1,4 dioxane (pure for synthesis) for all molecules tested, used at 10^{-3} M concentration.

2.1.7. Cyclic Voltammetry. Electrochemistry experiments were performed with a three-electrode setup using a platinum counter-electrode and a reference electrode. The reference electrode was an aqueous saturated calomel electrode with a salt bridge containing the supporting electrolyte. Ferrocene was added to the electrolyte solution at the end of each series of experiments, and the ferrocene/ferrocenium couple ($E^\circ = 0.405$ V/SCE in ACN–0.1 mol L⁻¹ Bu₄NBF₄) served as an internal probe. Potential values are given against the ferrocene/ferricinium couple. The working electrode was a glassy carbon disk (0.5 mm diameter). The electrode was carefully polished before each voltammetry experiment with 1 μ m diamond paste and 0.25 μ m alumina suspensions and ultrasonically rinsed in absolute ethanol. Electrochemical instrumentation consisted of a Tacussel GSTP4 programmer and of a home-built potentiostat equipped with a positive-feedback compensation device.¹⁹ The voltammograms were recorded with a 310 Nicolet oscilloscope. Oxygen was removed from all solutions by bubbling argon. The solvent was a toluene/acetonitrile mixture (50/50 v/v), and the supporting electrolyte was tetrabutylammonium tetrafluoroborate (Fluka, Puriss) at a concentration of 0.1 mol L⁻¹. Acetonitrile was from Merck (Uvasol quality less than 0.01% of water), and toluene was from Prolabo (R.P. Normapur).

2.1.8. Fabrication of OLED Device. The configuration of the device was ITO/CuPc/NPB/DPVBi:IV(1.2 wt %)/Alq3/LiF/Al. CuPc is copper phthalocyanine as a buffer layer, α -NPB is *N,N'*-bis(naphthalen-1-yl)-*N,N'*-bis(phenyl)benzidine as a hole transporting layer, DPVBi is 4,4'-bis(2,2-diphenylvinyl)-1,1'-biphenyl as a host, and Alq3 is tris(8-hydroxyquinolato) aluminum as an electron transporting layer. The EL device was fabricated as follows. ITO-coated glass substrates (with a sheet resistance of 20 Ω /square) were first cleaned by successive ultrasonic treatments in detergent (TDF4), deionized water, and ethanol. After that chemical cleaning, the substrates were treated by irradiation in a UV/Ozone chamber for 30 mn. The organic layers and the cathode LiF/Al were sequentially deposited by conventional vacuum vapor deposition in the same chamber without breaking the vacuum. The emissive layer of DPVBi:compound IV was made by coevaporation of the

two products from different sources. The I–V–L characteristics of the diodes were measured with a regulated power supply (ACT 100 Fontaine) combined with a multimeter (I–V) and a 1 cm² area silicon calibrated photodiode (Hamamatsu). The spectral emission (Commission Internationale de l'Eclairage (CIE) coordinates) was recorded with a spectrophotometer (SpectraScan PR650). All of the measurements were performed under ambient conditions.

2.2. Reagents. The synthesis and analytical characteristics of 2,3-methyl-5-bromopyridine (**1a**) and 2-methyl-5-bromopyridine (**1b**) have been previously reported.¹² 4-Hydroxybenzaldehyde (**6**), 4-cyanobenzaldehyde (**8**), 2-(2-thienyl)ethanol, 2,3-lutidine, 2-picolone, *tert*-butyldimethylsilyl chloride, tetrakis(triphenylphosphine)-palladium(0), *n*-butyllithium 2.5 M in hexane (all from Across), 2-isopropoxy-4,4,5,5-tetramethyl-1,3,2-dioxaborolane, *p*-toluene-sulfonic acid monohydrate (all from Aldrich), and 2-*n*-hexylthiophene (from Avocado) were used without further purification.

N,N-Dimethylformamide (DMF) was prepared by distillation over CaH₂ and degassed before reaction. Tetrahydrofuran (THF) was prepared by distillation over Na before reaction.

2.3. Syntheses. 5-(2-*tert*-Butyldimethyl-silanyloxy)-ethyl-thiophen-2-carboxaldehyde (**2**). *tert*-Butyldimethylsilyl chloride (4.22 g, 28 mmol) was added to a solution of 2(2-thienyl)ethanol (3.0 g, 23 mmol) and imidazole (1.9 g, 28 mmol) in DMF (11.5 mL, 150 mmol). The mixture was stirred at room temperature for 36 h. Filtration of the mixture was then carried out to eliminate a white precipitate (imidazolium chloride salt) followed by washing with diethyl ether. The organic layer was washed with water and dried over Na₂SO₄. The organic solvent was removed by evaporation under reduced pressure. 5.42 g (22.4 mmol) of a pure product was obtained (yield: 80%). ¹H NMR (CDCl₃) δ [ppm]: 0.00 (s, 6H), 0.85 (s, 9H), 3.03 (t, 2H), 3.82 (t, 2H), 6.83 (dd, 1H, ³J_{H,H} = 5.3 Hz, ⁴J_{H,H} = 1.27 Hz), 6.92 (t, 1H), and 7.11 (dd, 1H, ³J_{H,H} = 3.54 Hz, ⁴J_{H,H} = 1.27 Hz). ¹³C NMR (CDCl₃) δ [ppm]: 18.2, 25.9, 33.5, 64.1, 123.5, 125.1, 126.5, and 141.3.

To a solution of the previous protected compound (4 g, 16.5 mmol) in dry THF (80 mL) stirred at –78 °C was then added dropwise a solution of *n*-BuLi 2.5 M in hexane (7.24 mL, 18.1 mmol). The mixture was stirred at –78 °C for 2 h. DMF (165 mmol) was then added to the mixture stirred at room temperature for 12 h. The mixture was poured into water. The aqueous layer was extracted with diethyl ether, and the combined diethyl ether layers were washed with water and dried over Na₂SO₄. The solvent was removed under reduced pressure. 4.0 g (14.8 mmol) of a pure yellow product (**2**) was obtained (yield: 90%). ¹H NMR (CDCl₃) δ [ppm]: 0.00 (s, 6H), 0.86 (s 9H), 3.03 (t, 2H), 3.82 (t, 2H), 6.92 (d, 1H, ³J_{H,H} = 3.54 Hz), 7.59 (d, 1H, ³J_{H,H} = 3.79 Hz), and 9.79 (s, 1H). ¹³C NMR (CDCl₃) δ [ppm]: 18.1, 25.7, 34.2, 63.1, 126.1, 136.6, 142.1, 153.4, and 182.6.

2-(3-Methyl-5-bromo-pyridin-2-yl)-1-(5-(2-(*tert*-butyl-dimethyl-silanyloxy)-ethyl)-thiophen-2-yl)-ethanol (**4**). To a solution of diisopropylamine (3.93 mL, 28 mmol) in dry THF (130 mL) stirred at –20 °C under argon was added dropwise a solution of *n*-BuLi 2.5 M in hexane (11 mL, 27.5 mmol). The mixture was stirred at –20 °C for 20 min. The 2,3-dimethyl-5-bromopyridine (**1a**) (4.94 g, 26.5 mmol) was then added. The resulting red mixture was stirred at –20 °C, under argon, for 2 h, and compound **2** (7.17 g, 26.5 mmol) was added. The stirring was kept under argon for 12 h. The reaction was quenched into water. The aqueous layer was extracted with diethyl ether, and the combined organic layers were washed with water and dried over Na₂SO₄. The solvent was removed under reduced pressure. The crude product was purified by washing in hexane. 8.46 g (18.5 mmol) of a solid white pure product was obtained (yield: 70%). ¹H NMR (CDCl₃) δ [ppm]: 0.00 (s, 6H), 0.87 (s, 9H), 2.22 (s, 3H), 2.99 (t, 2H), 3.79 (t, 2H), 5.41–5.51

(m, 3H), 6.66 (d, 1H, $^3J_{\text{H,H}} = 3.28$ Hz), 6.77 (d, 1H, $^3J_{\text{H,H}} = 3.54$ Hz), 7.6 (d, 1H, $^4J_{\text{H,H}} = 2.03$ Hz), and 8.4 (d, 1H, $^4J_{\text{H,H}} = 2.02$ Hz), ^{13}C NMR (CDCl_3) δ [ppm]: -5.4, 18.3, 18.5, 25.9, 33.8, 41.8, 64.2, 68.7, 118.3, 122.9, 124.6, 133.9, 140.2, 140.5, 145.7, 146.8, and 156.5.

[4-(tert-Butyl-dimethyl-silanyloxy)-benzylidene]-phenyl-amine (7). Aniline (5.75 mL, 63.5 mmol) was added to a solution of 4-hydroxybenzaldehyde (7.0 g, 57.4 mmol) in toluene (300 mL). The mixture was refluxed for 24 h. During the reaction, water was trapped in Dean–Stark. The imine precipitated during formation. This precipitate was filtered and dried under reduced pressure. 11.2 g (56.8 mmol) of a pure white product was obtained (yield: 99%). ^1H NMR ($\text{DMSO}-d_6$) δ [ppm]: 6.88 (d, 2H, $^3J_{\text{H,H}} = 8.63$ Hz), 7.18 (m, 3H), 7.36 (d, 2H, $^3J_{\text{H,H}} = 8.63$ Hz), and 8.43 (s, 1H). ^{13}C NMR ($\text{DMSO}-d_6$) δ [ppm]: 166.0, 121.2, 125.7, 127.9, 129.5, 131.0, 152.4, 160.4, 161.0. Anal. Calcd for $\text{C}_{13}\text{H}_{11}\text{NO}$: C, 79.16; H, 5.62; N, 7.10; O, 8.11. Found: C, 79.13; H, 5.60; N, 7.12; O, 8.71.

tert-Butyldimethylsilyl chloride (2.53 g, 17 mmol) was then added to a solution of **6** (2.53 g, 17 mmol) and imidazole (3.0 g, 15.2 mmol) in DMF (10 mL). The mixture was stirred at room temperature for 36 h. Filtration of the mixture was then carried out to eliminate a white precipitate (imidazolium chloride salt) followed by washing with diethyl ether. The organic layer was washed with water and dried over Na_2SO_4 . The organic solvent was removed by evaporation under reduced pressure. 3.3 g (10.6 mmol) of a pure product was obtained (yield: 70%). ^1H NMR (CDCl_3) δ [ppm]: ^1H NMR (CDCl_3) ppm: 0.27 (s, 6H), 1.03 (s, 9H), 6.95 (d, 2H, $^3J_{\text{H,H}} = 11.4$ Hz), 7.24 (m, 3H), 7.41 (t, 2H), 7.82 (d, 2H, $^3J_{\text{H,H}} = 11.4$ Hz), and 8.41 (s, 1H). ^{13}C NMR (CDCl_3) δ [ppm]: -4.4, 18.2, 25.6, 120.4, 127.8, 125.5, 129.0, 129.7, 130.3, 152.3, 158.7, and 159.7.

5-Bromo-3-methyl-2-(2-(5-(2-(tert-butyl-dimethyl-silanoxy)-ethyl)-thiophen-2-yl)-vinyl)-pyridine (Br1). A solution of compound **4** (8.46 g, 18.5 mmol) and *p*-toluenesulfonic acid (351.5 mg, 1.85 mmol) in toluene (350 mL) was stirred at 120 °C for 4 h. The mixture was cooled to room temperature, and the solvent was removed under reduced pressure. The crude product was soluble in dichloromethane. The dichloromethane layer was washed with water and dried over Na_2SO_4 . The crude product was precipitated twice from hexane. 6.4 g (14.5 mmol) of a pure white solid was obtained (yield: 80%). Mp = 61.9 °C. ^1H NMR (CDCl_3) δ [ppm]: 0.00 (s, 6H), 0.87 (s, 9H), 2.35 (s, 3H), 2.99 (t, 2H), 3.83 (t, 2H), 6.73 (d, 1H, $^3J_{\text{H,H}} = 3.53$ Hz), 6.91 (d, 1H, $^3J_{\text{H,H}} = 15.41$ Hz), 7.0 (d, 1H, $^3J_{\text{H,H}} = 3.53$ Hz), 7.56 (d, 1H, $^4J_{\text{H,H}} = 2.02$ Hz), 7.81 (d, 1H, $^3J_{\text{H,H}} = 15.41$ Hz), and 8.43 (d, 1H, $^4J_{\text{H,H}} = 2.02$ Hz). ^{13}C NMR (CDCl_3) δ [ppm]: -5.4, 18.3, 18.5, 25.9, 34.1, 63.8, 117.9, 121.2, 126.2, 127.6, 128.3, 131.9, 140.1, 140.7, 142.5, 147.9, and 152.0. Anal. Calcd for $\text{C}_{20}\text{H}_{28}\text{NOSBrSi}$: C, 54.78; H, 6.44; N, 3.19; S, 7.31. Found: C, 54.68; H, 6.43; N, 3.23; S, 7.46.

5-Bromo-2-(2-[4-(tert-butyl-dimethyl-silanyloxy)-phenyl]-vinyl)-3-methyl-pyridine (Br3). To a solution of diisopropylamine (1.54 mL, 11.0 mmol) in dry THF (45 mL) stirred at -20 °C under argon was added dropwise a solution of *n*-BuLi 2.5 M in hexane (4.24 mL, 10.6 mmol). The mixture was stirred at -20 °C for 20 min. 2,3-Dimethyl-5-bromopyridine (**1a**) (1.79 g, 9.64 mmol) was then added. The resulting red mixture was stirred at -20 °C, under argon, for 2 h, and compound **7** (3.0 g, 9.64 mmol) was added. The stirring was kept under argon for 12 h. The reaction was quenched into water. The aqueous layer was extracted with diethyl ether, and the combined organic layers were washed with water and dried over Na_2SO_4 . The solvent was removed under reduced pressure. The crude product was purified by washing with hexane. 2.2 g (5.46 mmol) of a pure white solid was obtained (yield: 57%). ^1H NMR (CDCl_3) δ [ppm]: 0.20 (s, 6H), 0.97 (s, 9H), 2.38 (s, 3H), 6.82 (d,

2H, $^3J_{\text{H,H}} = 8.33$ Hz), 7.08 (d, 1H, $^3J_{\text{H,H}} = 15.42$ Hz), 7.45 (d, 2H, $^3J_{\text{H,H}} = 8.32$ Hz), 7.56 (d, 1H, $^4J_{\text{H,H}} = 1.54$ Hz), 7.70 (d, 1H, $^3J_{\text{H,H}} = 15.42$ Hz), and 8.45 (d, 1H, $^4J_{\text{H,H}} = 1.54$ Hz).

4-(2-(5-Bromo-3-methyl-pyridin-2-yl)-vinyl)-benzonitrile (Br4). 2,3-Dimethyl-5-bromopyridine (**1a**) (4.255 g, 22.9 mmol), 4-cyanobenzaldehyde (**8**) (3 g, 22.9 mmol), and *p*-toluenesulfonic acid (0.805 g, 4.58 mmol) were blended. The mixture was then stirred at 160 °C. After 36 h, the mixture was cooled to room temperature and washed with brine. The aqueous layer was extracted with dichloromethane. The resulting organic layer was washed with water and dried over Na_2SO_4 . The solvent was removed under reduced pressure. The crude product was purified by three washings with acetone. 2.14 g (7.16 mmol) of a clear powder was obtained (yield: 31%). ^1H NMR ($\text{DMSO}-d_6$) δ [ppm]: 2.45 (s, 3H), 7.35 (d, 1H, $^3J_{\text{H,H}} = 15.7$ Hz), 7.65 (m, 5H), 7.79 (d, 1H, $^3J_{\text{H,H}} = 15.7$ Hz), and 8.52 (d, 1H, $^4J_{\text{H,H}} = 2.3$ Hz). ^{13}C NMR ($\text{DMSO}-d_6$) δ [ppm]: 17.8, 110.7, 118.1, 118.7, 125.7, 126.7, 126.9, 127.1, 131.6, 132.1, 139.6, 140.0, 140.5, 147.3, 147.7, and 150.4. Anal. Calcd for $\text{C}_{15}\text{H}_{11}\text{N}_2\text{Br}$: C, 60.22; H, 3.71; N, 9.36; Br, 26.71. Found: C, 60.23; H, 3.64; N, 9.39; Br, 26.62.

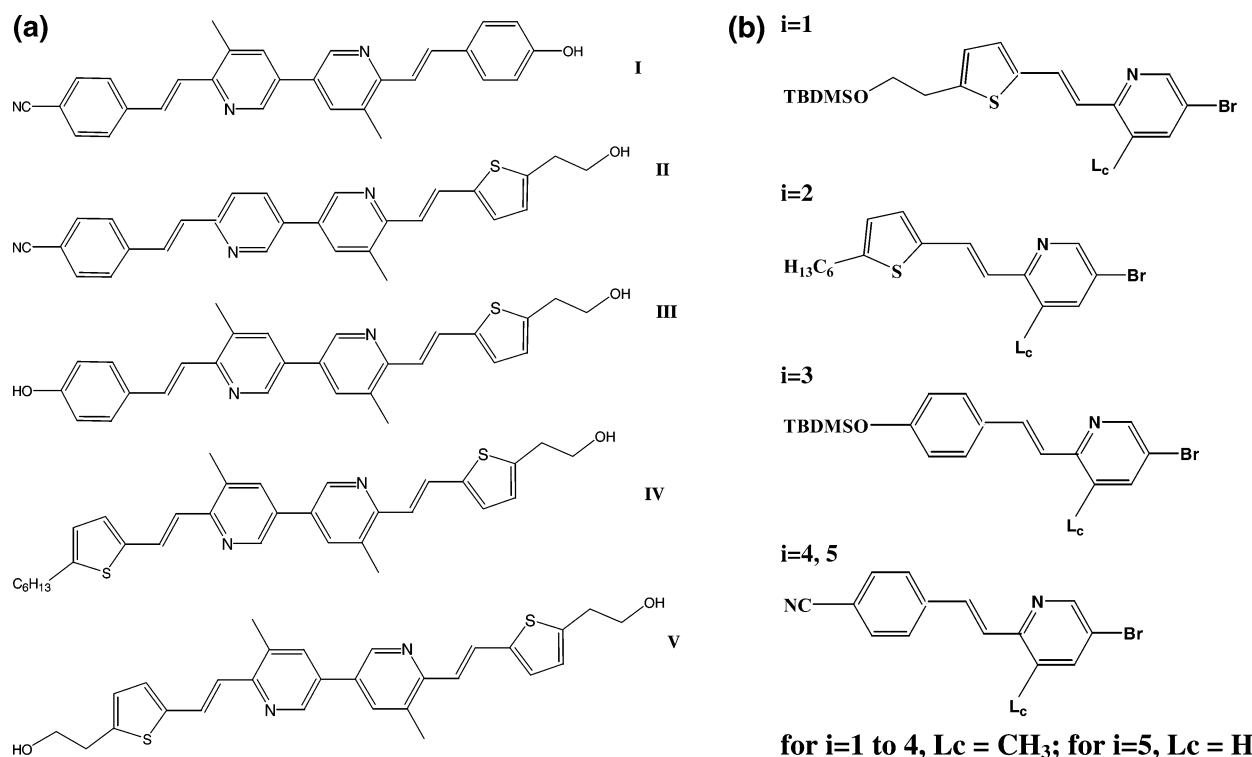
2-(2-(5-(2-(tert-Butyl-dimethyl-silanoxy)-ethyl)-thiophen-2-yl)-vinyl)-3-methyl-5-(4,4,5,5-tetramethyl-[1,3,2]dioxaborolan-2-yl)-pyridine (B1). To a solution of compound **Br1** (9.62 g, 22.6 mmol) in dry THF (170 mL) stirred at -78 °C under argon was added dropwise a solution of *n*-BuLi 2.5 M in hexane (9.16 mL, 22.9 mmol). The mixture was stirred at -78 °C for 20 min. 2-Isopropoxy-4,4,5,5-tetramethyl-1,3,2-dioxaborolane (4.73 mL, 23.2 mmol) was then added, and the stirring was kept at -78 °C for 2 h. The mixture was warmed slowly to -35 °C and stirred at this temperature for 1 h. The mixture was poured into water. The aqueous layer was extracted with diethyl ether, and the combined diethyl ether layers were washed with water and dried over Na_2SO_4 . The solvent was removed under reduced pressure. The crude product was purified by filtration on silica (chloroform–ethyl acetate 9:1) yielding pure compound **B1** (9.97 g, 20.5 mmol) in 91% yield as a yellowish oil. ^1H NMR (CDCl_3) δ [ppm]: 0.00 (s, 6H), 0.87 (s, 9H), 1.36 (s, 12H), 2.37 (s, 3H), 2.99 (t, 2H), 3.83 (t, 2H), 6.75 (d, 1H, $^3J_{\text{H,H}} = 3.54$ Hz), 7.04 (d, 1H, $^3J_{\text{H,H}} = 15.16$ Hz), 7.02 (d, 1H, $^3J_{\text{H,H}} = 3.54$ Hz), 7.81 (d, 1H, $^4J_{\text{H,H}} = 1.77$ Hz), 7.92 (d, 1H, $^3J_{\text{H,H}} = 15.41$ Hz), and 8.75 (d, 1H, $^4J_{\text{H,H}} = 1.77$ Hz). ^{13}C NMR (CDCl_3) δ [ppm]: -5.9, -5.2, 18.1, 18.4, 24.5, 24.8, 25.7, 33.9, 63.7, 83.8, 122.0, 125.8, 126.1, 128.1, 129.3, 140.8, 142.3, 144.1, 144.5, 152.4, and 155.2.

Suzuki Cross-Coupling, General Procedure. Dioxaborolane derivative **B(j)**, bromide derivative **Br(i)**, and $(\text{PPh}_3)_4\text{Pd}(0)$ (0.5–2.0 mol %) were dissolved in a mixture of THF ($[\text{B(j)}] = [\text{Br(i)}] = 0.4$ M) and aqueous 2 M K_2CO_3 (1:1.5 THF). The solution was first put under argon atmosphere and was heated at 80 °C with vigorous stirring for 48 h. After transfer in a separatory funnel, the aqueous layer was extracted with dichloromethane and the combined dichloromethane layers were then washed with water and dried over Na_2SO_4 . The solvent was removed under reduced pressure.

3. Results and Discussion

3.1. Synthesis. The structures of the π -conjugated chromophores (**I–V**) are shown in Chart 1a. They were obtained as sketched in Figure 1. The intermediate key compounds (Chart 1b) were synthesized according to Scheme 1A and B. The starting materials, 2,3-dimethyl-5-bromopyridine (**1a**) and 2-methyl-5-bromopyridine (**1b**), were prepared as described previously.²⁰ The hydroxyl group of functionalized aldehydes (**2**, **6**) was protected with TBDMS, which was

Chart 1



chosen because it tolerates later lithiation. The hydroxy-functionalized derivative **2** was obtained by formylation, with *n*-butyllithium (*n*-BuLi) and DMF, of the protected 2-(2-thienyl)ethanol, whereas the 5-hexyl-2-thiophenecarboxaldehyde (**3**) was obtained by formylation (Vilsmeier–Haack reaction) of 2-thiophenecarboxaldehyde. The detailed procedure is reported in the Experimental Section.

The synthetic approach to prepare the target chromophores is based on the Suzuki coupling of 6-substituted-3-bromopyridine and 6-substituted-3-pyridylboronic ester building blocks (Figure 1). According to this methodology, several 6-substituted-3-bromopyridine building blocks were synthesized (Scheme 1A). Three different routes were used, depending on the electron-donor or electron-acceptor character of the end substituent. For the building blocks bearing an electron-rich ring (**Br1–2**) or an electron-acceptor group (**Br3**), a pathway adapted from a procedure reported in the literature for symmetrical 4,4'-disubstituted-2,2'-bipyridines²¹ was defined (Scheme 1Aa). Reaction of **1a** with lithium diisopropylamide (LDA) generated the red-colored lithioanion, which reacted with the appropriate aldehyde to give the corresponding alcohol (**4–5**). Subsequent treatment with *p*-toluenesulfonic acid produced the respective π -conjugated 6-substituted-3-bromopyridine building blocks **Br1–2** in 80–85% yield on the 10–20 g scale. Only the *trans* isomer was obtained.

To avoid the thermal dehydration step, another route based on an adaptation of the Siegrist reaction was used (Scheme

1Ab). The Siegrist method is a condensation of an aryl imine and the methyl group of an aromatic ring, mainly phenyl ring, in the presence of a base, as for example *t*-BuOK, allowing the formation in a one-pot operation of a *trans*-stilbene derivative.²² We extended this reaction, for the first time at our knowledge, to a pyridinic ring (2,3-dimethyl-5-bromopyridine) bearing the activated methyl group in the ortho position to the nitrogen atom. As an example, the synthesis of Br3 is reported. First, the condensation of the *p*-hydroxybenzaldehyde (**6**) with aniline in refluxing toluene afforded benzaldimine in an overall 99% yield. Protection of the hydroxyl group with *tert*-butyldimethylsilyl group provided protected benzaldimine (**7**). Treatment of the **1a** with **7** in the presence of LDA, instead of *t*-BuOK, in THF at –20 °C gave **Br3** in 60% yield on the 5–10 g scale. As expected, examination of the ¹H NMR spectra of the product showed that only the *trans*-isomer was obtained.

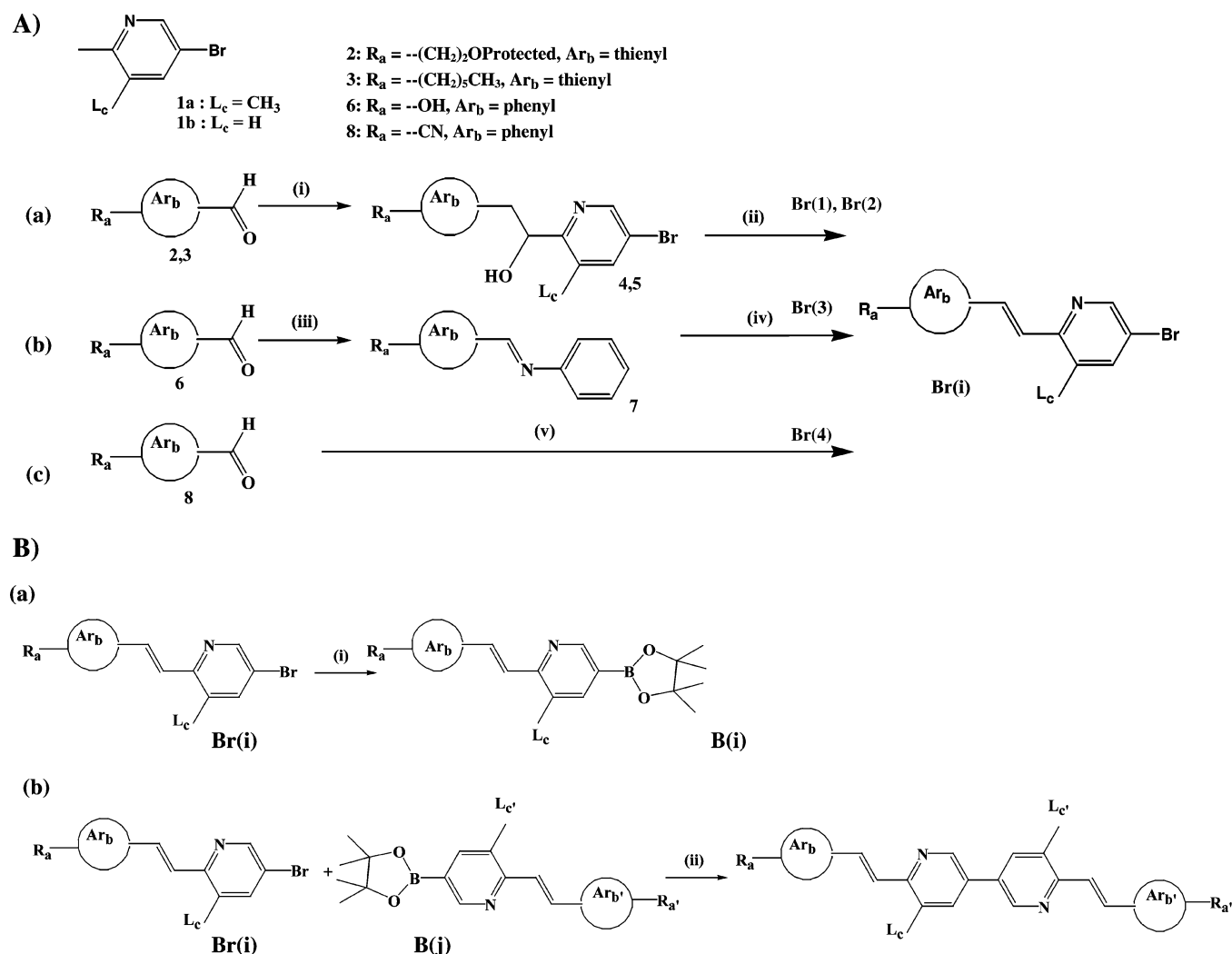
As the presence of the cyano group precludes the use of these two general procedures in the case of *para*-cyanobenzaldehyde, building blocks **Br4–5** have been obtained in reasonable yield (31%) from the one-step Knoevenagel-type condensation reaction in acidic medium of **8** with **1a** and **1b**, respectively (Scheme 1Ac). The exclusive presence of the *trans*-vinylene unit is clearly evidenced by the three-bonds coupling constant (³J_{H,H} 16 Hz) in ¹H NMR spectra.

As our synthetic approach was based on the nonsymmetric Suzuki-type transition metal-catalyzed cross-coupling, some of the previous building blocks needed to be functionalized (borylation according to Scheme 1Ba) in a way that they could be used as building blocks in this reaction (Scheme

(20) (a) Pearson, D. E.; Hargrove, W. W.; Chow, J. K. T.; Suthers, B. R. *J. Org. Chem.* **1961**, 26, 789. (b) Bonnier, J. M.; Court, J. *Bull. Soc. Chim. Fr.* **1970**, 1, 142.

(21) (a) Juris, A.; Campagna, S.; Bidd, I.; Lehn, J.-M.; Ziessel, R. *Inorg. Chem.* **1988**, 27, 4007. (b) Maury, O.; Guégan, J.-P.; Renouard, T.; Hilton, A.; Dupau, P.; Sandon, N.; Toupet, L.; Le Bozec, H. *New J. Chem.* **2001**, 25, 1553.

(22) (a) Siegrist, A. E.; Liechti, P.; Meyer, H. R.; Weber, K. *Helv. Chim. Acta* **1969**, 52, 2521. (b) Zerban, G.; Meier, H. *Z. Naturforsch., B: Chem. Sci.* **1993**, 48, 171. (c) Skibniewski, A.; Bluet, G.; Druzé, N.; Riant, O. *Synthesis* **1999**, 3, 459–462.

Scheme 1^a

^a Reagents and conditions (A): (i) LDA, THF, -20°C , **1a** (**1b**), 2 h, **2** or (**3**), -20°C to room temperature, 12 h; (ii) toluene, *p*-toluenesulfonic acid, reflux, 4 h; (iii) aniline, toluene, **6**, reflux, Dean–Stark trap, 24 h; (iv) LDA, THF, -20°C , **1a**, 2 h, **7**, -20°C to room temperature, 12 h; (v) DMF, **1a**, *p*-toluenesulfonic acid, 170°C , 10 h. ^b Reagents and conditions (B): (i) *n*-BuLi, THF, -78°C , dioxaborolane, 2 h, -35°C , 1 h; (ii) THF, K_2CO_3 , $(\text{PPh}_3)_4\text{Pd}$, 80°C , 48 h; (iii) HF, THF, 5 h.

1Bb). The incorporation of the coupling functionality (boronic acid diester function) involves (i) the regioselective lithiation at position 3 of the appropriate 3-bromopyridine-based building block followed by adaptation of standard procedures, described for borylation of aryl halides, for (ii) the introduction of boronic diesters.^{15c} As examples, building blocks **Br1–3** were converted to boronated building blocks **B1–3**, respectively, upon reaction with *n*-BuLi and 2-isopropoxy-4,4,5,5-tetramethyl-1,3,2-dioxaborolane in anhydrous THF, in a 90% yield and a multigram scale after purification. However, it should be noted that this route is not available for building blocks bearing the electron-withdrawing cyano group because of the sensitivity of this one toward *n*-BuLi.

As our main aim was to use the palladium-catalyzed Suzuki cross-coupling for the preparation of various π -conjugated 6,6'-disubstituted-3,3'-bipyridine derivatives, five representative chromophores (**I–V**) have been synthesized by adapting standard procedures (Scheme 1Bb). First, two push–pull chromophores (**I** and **II**) have been synthesized. Whereas **I** was also obtained previously by another route,^{12c}

II was a new compound which enlightened the present strategy. Indeed, all of the various parameters (terminal and lateral substituents as well as aromatic rings) of the two starting building blocks were different. The brominated building blocks bearing an electron-withdrawing group (**Br4–5**) were coupled with various pyridylborane-based building blocks bearing an electron-donating group (**B3** and **B1**), giving, after deprotection, push–pull chromophores (**I**) and (**II**), respectively. Second, two other kinds of nonsymmetrical compounds (**III** and **IV**) were prepared. In **III**, the acceptor central core (A–A) is sandwiched between two different electron-donor groups (D and D'), leading to a D–A–A–D' structural motif. It should be noted that the coupling either of **Br1** with **B3** or of **Br3** with **B1** gave the chromophore **III**. On the other hand, whereas in **IV** the two electron-donor groups are identical, the dissymmetry is the result of the terminal substituents, the building blocks being either **Br(2)** and **B(1)** or **Br(1)** and **B(2)**. Third, as an extension of our modular strategy, the symmetrical chromophore **V** was also synthesized, resulting from the cross-coupling of **Br1** and **B1**, leading to a D–A–A–D structural

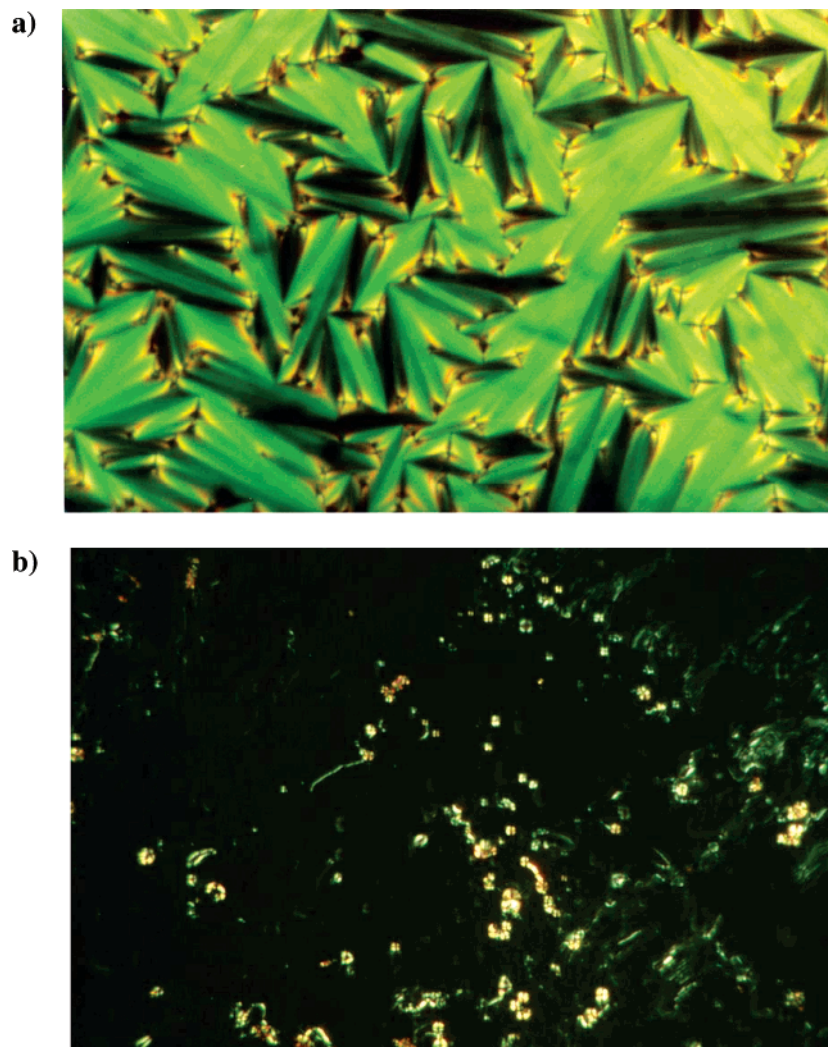


Figure 2. Optical texture of **II** mounted between two glass slides: (a) not modified, (b) modified with an alkoxy silane.

motif. All of these chromophores bearing one hydroxyl group could be grafted as a side-group, onto a polymer backbone. **V** could be used as a difunctional monomer and introduced in a main-chain polymer. All of these compounds had spectral data consistent with the assigned structure.

3.2. Mesomorphic Behavior. The thermal behavior was examined by DSC, and phase assignments were based on powder X-ray diffraction (XRD) and polarized-light optical microscopy (POM). The transition temperatures, phase sequence, and thermodynamic data of **II** are listed in Table 1.

Table 1. Thermodynamic Data and Phase Sequence of **II**

phase, transition temp (°C), [enthalpy changes ΔH (kJ mol ⁻¹)] ^a
first heating
K ₁ , 98.8, [~ -4]; K ₂ , 146.7, [~ 35.3], LC, 230.4, [~ 2.4], I

^a Determined by DSC. K₁, K₂, LC, and I: see text.

As reported previously,¹² the 6,6'-distyryl-3,3'-bipyridine derivatives form easily mesophases. As liquid-crystalline properties of push-pull molecules are of interest for NLO,^{11,12} the mesogenic properties of chromophore **II** have been investigated and compared to those of **I**. The CN group and the alkyl group are known to favor the formation of nematic and smectic phases, respectively.²³ This was observed with **I**,¹² which forms smectic (S_B and S_A), nematic

(N), and isotropic phases. The S/N and N/I transition appears at high temperatures (233.7 and 302.5 °C).

DSC evidences that compound **II**, in which one phenyl group is replaced by a thienyl ring, exhibits during heating the following phase sequence: (i) an exothermic broad peak ($\Delta H \approx -3.4$ kJ mol⁻¹) at 98.8 °C, corresponding to crystallization into another crystalline phase (K₁/K₂ transition), (ii) melting of this second phase into a liquid-crystalline (LC) phase at 146.7 °C ($\Delta H \approx 35.3$ kJ mol⁻¹), and (iii) clearing of the mesophase into the isotropic liquid at 230.4 °C ($\Delta H \approx 2.4$ kJ mol⁻¹).

Figure 2a presents the mesomorphic texture of compound **II** observed under a polarizing microscope. Above its first melting point, **II** gives a clear focal-conic fan texture, which exhibits characteristic features of a smectic phase. Upon further heating, the sample clears directly into isotropic liquid without showing additional mesophase. To discriminate the type of the mesophase, the sample was mounted between two glass slides, which were modified with an alkoxy silane (octadecyltrichlorosilane) usually used to induce an alignment of the liquid crystal chains perpendicular to the surface substrate. As shown in Figure 2b, no birefringence was

(23) *Handbook of Liquid Crystals*; Demus, D., Goodby, J., Gray, G. W., Spiess, H.-W., Vill, V., Eds.; Wiley-VCH: Weinheim, 1998.

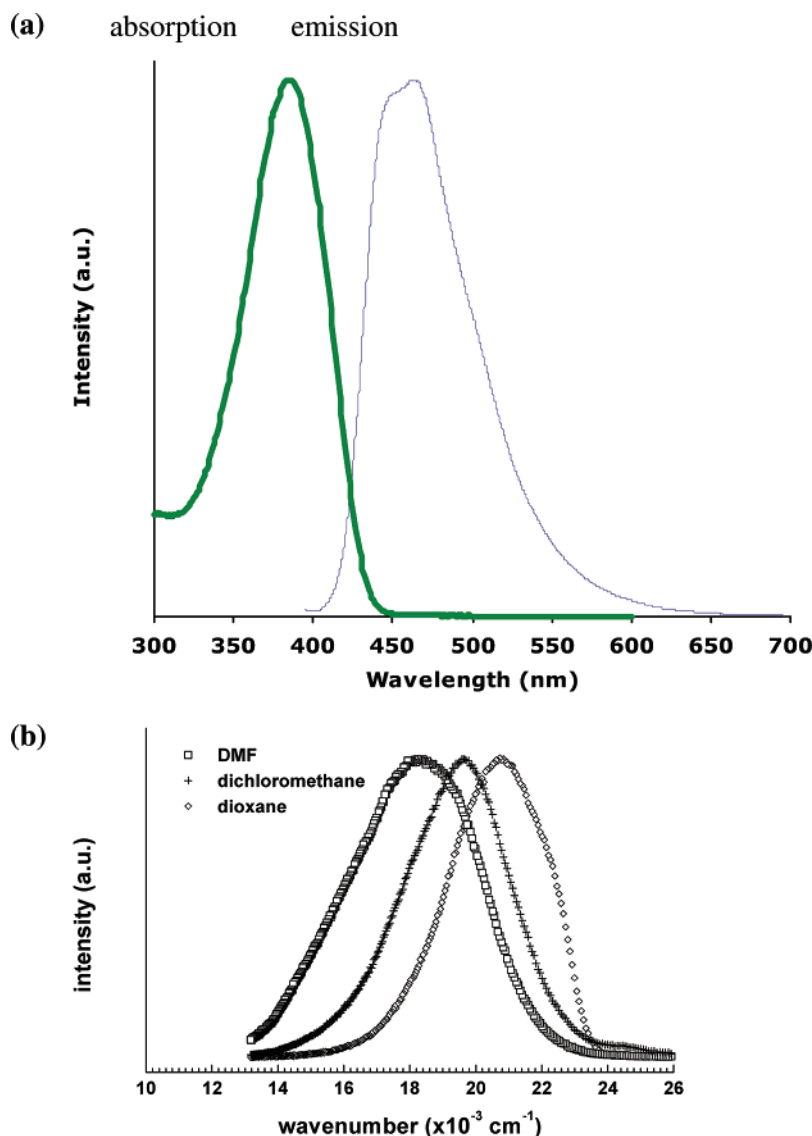


Figure 3. (a) Absorption and emission spectra of **IV** in dichloromethane. (b) Emission spectra of **I** in DMF, dichloromethane, and dioxane.

observed. This is characteristic of the perfect homeotropic arrangement of a smectic A mesomorphic state.

The X-ray diffraction pattern of the mesophase, recorded at 180 °C, consists of (i) a broad diffuse scattering halo in the wide angle region, at ~ 5.81 Å, and a single sharp and intense reflection in the small angle region, at ~ 48.76 Å. These reflections are related, respectively, to an average molecular width and to the layer thickness d . The lamellar spacing (d) is larger than the extended molecular length ($L = 25.13$ Å); the ratio d/L is on the order of 1.9, which suggests an interdigitated bilayer structure due to the terminal strong polar cyano group.²³

On the contrary, compounds **III**, **IV**, and **V** do not exhibit any mesomorphism. This feature could be explained by the absence of a strong polar group (CN) and/or long alkyl chains.²³

3.3. Optical Properties. All linear optical measurements (i.e., absorption and emission spectra) were performed in solution in a wide range of solvent polarity (from $\epsilon = 2.21$ for dioxane to $\epsilon = 46.45$ for DMSO).

Absorption. For all compounds, the absorption maxima (λ_{max}) in dichloromethane are reported in Table 1S. No

noticeable solvatochromic shift is observed for all of the chromophores. The values of λ_{max} lie in the range of 372 nm for **I** to 391 nm for **IV** and **V**, which are identical from the electronic point of view. A representative absorption spectrum is displayed in Figure 3a in the case of chromophore **IV**. The main features of the spectra are an intense, low-lying (near the UV region) absorption band. The large molar absorption coefficients (values of $\epsilon > 50\,000$ L mol⁻¹ cm⁻¹) are indicative of highly π -conjugated systems.

Photoluminescence. All of the compounds exhibit intense fluorescence. Two distinct behaviors are observed depending on the electronic structure of the chromophores.

For both push–pull chromophores (**I** and **II**), solvent polarity influences emission properties. As illustrated in Figure 3b for compound **II**, a large bathochromic shift (4500 cm⁻¹ for **I** and 3200 cm⁻¹ for **II**) of the emission maxima (λ_{em}) is observed when dioxane is replaced by DMSO, and dioxane is replaced by DMF for **I** and **II**, respectively. This pronounced positive solvatochromism with increasing polarity of the solvent, as well as the large Stokes shift values, indicate that a significant conformational change occurs upon excitation as a result of a significant electronic redistribution

leading to the highly polar excited state. This is attributed to an intramolecular charge-transfer (ICT) state involving charge separation within the whole molecule, inducing consequently a large dipole moment for the excited state, and NLO properties as observed for the other push–pull chromophores of this series.^{12c}

On the other hand, the D–A–A–D-type chromophores (**III**, **IV**, and **V**) do not exhibit solvatochromism. The main feature of the representative emission spectrum reported in Figure 3a for compound **IV** is a broad structured emission with two distinct peaks at 453 and 467 nm.

Relation between Photoluminescence and NLO Properties. Oudar and Chemla have shown that push–pull compounds having a low-lying high-intensity ICT transition, associated with a large change in dipole moment, yield quadratic hyperpolarizabilities.²⁴ In a previous paper,^{12c} we proposed the estimate of the static hyperpolarizability (β_0) in a simple way based on (i) the characteristics of the absorption band (oscillator strength and transition energy), and (ii) the solvatochromism of the emission band. It was shown that the evaluated value for **I** was consistent with the experimental value determined by EFISHG measurements. In the present work, as **I** and **II** exhibit the same optical behavior (in absorption and emission), on one hand, and the thienyl group is a weak donor group on the other one, the NLO properties of **II** should be similar to the ones measured previously for **I** ($\mu\beta \approx 150 \times 10^{-48}$ esu, $\mu\beta_0 \approx 100 \times 10^{-48}$ esu, and $\beta_0 \approx 20 \times 10^{-30}$ esu). Despite that these values are 2 orders of magnitude lower than the ones obtained for 2-dicyanomethylen-3-cyano-4,5,5-trimethyl-2,5-dihydrofuran (TCF)-based chromophores,⁷ these results are promising for the following reasons. First, our synthetic strategy has allowed us to successfully synthesize NLO liquid crystal chromophores exhibiting enhanced hyperpolarizabilities as compared to typical NLO active mesogenic compounds reported in the literature ($\beta_0 \approx 5 \times 10^{-30}$ to 30×10^{-30} esu).^{12c} Second, because of our convergent approach, it should be possible (i) to synthesize building blocks bearing stronger electron acceptors and electron donor groups, and (ii) to couple them to obtain more efficient NLO chromophores.

3.4. Laser Emission. Laser emission was obtained from all of the chromophores. Preliminary results will be presented here, for example, for the blue emitting chromophores **I** and **V**. Complete results will be given elsewhere. The spectral profiles of the emission from **I**, taken at several pump intensities, are shown in Figure 4a. When the dyes were photopumped at low intensities, below 0.1 mJ/pulses, only spontaneous emission was observed. Pumping at higher power densities resulted in a narrowing of the emission spectrum, and laser emission became evident, the full width at half-maximum (fwhm) of the spectra dropping to 1.8 nm. Similar results were obtained for **V**. The lasing properties have been compared to the ones of Coumarin 540A, a standard dye emitting in the same range. Under the same experimental conditions (optical cavity, temporal width pulse, solvent), by pumping at 337 nm, Coumarin 540A at 2×10^{-2} M exhibits²⁵ an energy conversion efficiency of 32%

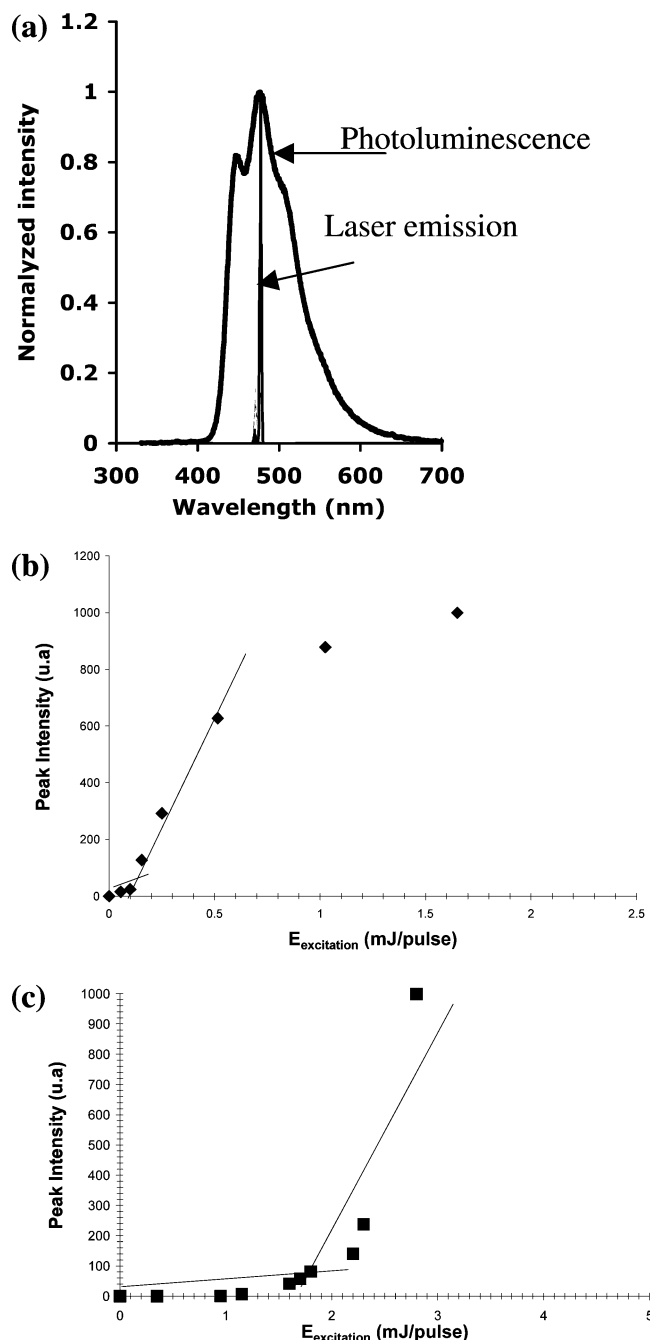


Figure 4. Laser emission threshold for (a) **I**, (b) **V**.

at 1.2 mJ/pulse. The comparison was made above the laser threshold (2 mJ/pulse) and reported that Coumarin 540 A is only 2 times more intense than **I** and **V**. This result suggested that **I** and **V** have noticeable lasing performances. Finally, the laser emission threshold is deduced by a brutal breakdown²⁶ in the curve of peak intensity in accordance with photopumped intensities. The laser emission thresholds are 0.1 and 1.8 mJ/pulses for **I** and **V**, respectively. The laser emission threshold for **I**, in Figure 4b, is low enough and shows a saturation effect for higher photopumped intensities. We noticed that there is no saturation for **V** in Figure 4c.

3.5. Electrochemical Study. In view of the potential application of such molecules in optoelectronics, it is

(25) Costela, A.; Garcia-Moreno, I.; Barroso, J.; Sastre, R. *J. Appl. Phys.* **1998**, 83, 650.

(26) Tessler, N. *Adv. Mater.* **1999**, 11, 363.

(24) Oudar, J. L.; Chemla, D. S. *J. Chem. Phys.* **1977**, 66, 2664.

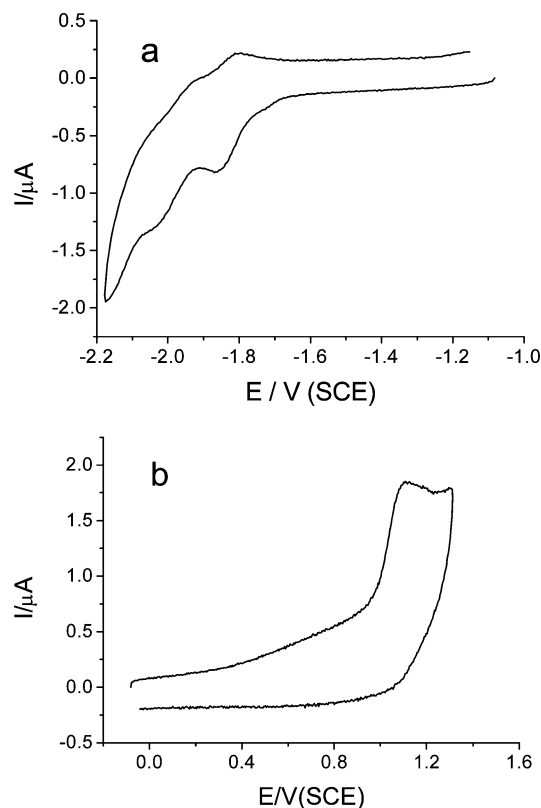


Figure 5. Cyclic voltammetry of **IV** in a toluene/acetonitrile mixture (50/50 v/v) containing 0.1 mol L^{-1} NBu_4BF_4 as supporting electrolyte on a 0.5 mm diameter disk glassy carbon electrode: (a) reduction and (b) oxidation voltammograms. Concentration = $1.4 \times 10^{-3} \text{ mol L}^{-1}$; scan rate = 0.2 V s^{-1} ; $T = 20^\circ\text{C}$.

important to consider their energy gap $-\Delta E_g$ — and the relative ionization potential (IP) and electron affinity (EA), parameters that indicate the facility to inject holes and electrons, respectively, in the material. These values can be estimated from the first oxidation and first reduction potentials in solution (E_{ox}° and E_{red}°), which are associated with the highest occupied and the lowest unoccupied molecular orbitals (HOMO and LUMO energy levels, respectively).²⁷ For this purpose, the electrochemical behavior was investigated by cyclic voltammetry (CV), to measure the redox potentials, and thus to determine the energy gap (that can be estimated from the electrochemical gap $\Delta E_{g,\text{elec}} = E_{\text{ox}}^\circ - E_{\text{red}}^\circ$), IP, and EA.

Only the electrochemical oxidation and reduction of the blue emitting chromophore **IV** have been investigated in view to elaborate an emitting device. Typical voltammograms of the reduction and oxidation are presented in Figure 5a and b, respectively.

In reduction (Figure 5a), the studied compound presents two monoelectronic transfers. The first reduction process was reversible at low scan rate (0.2 V s^{-1}), showing a relatively good chemical stability of the radical-anion (lifetime higher than 10 s). In these conditions, the second process can be unambiguously ascribed to the reduction of the radical anion to the corresponding dianion. From this reversible voltammogram, the formal potential E_{red}° for the first reduction was immediately derived as the half-sum between the forward

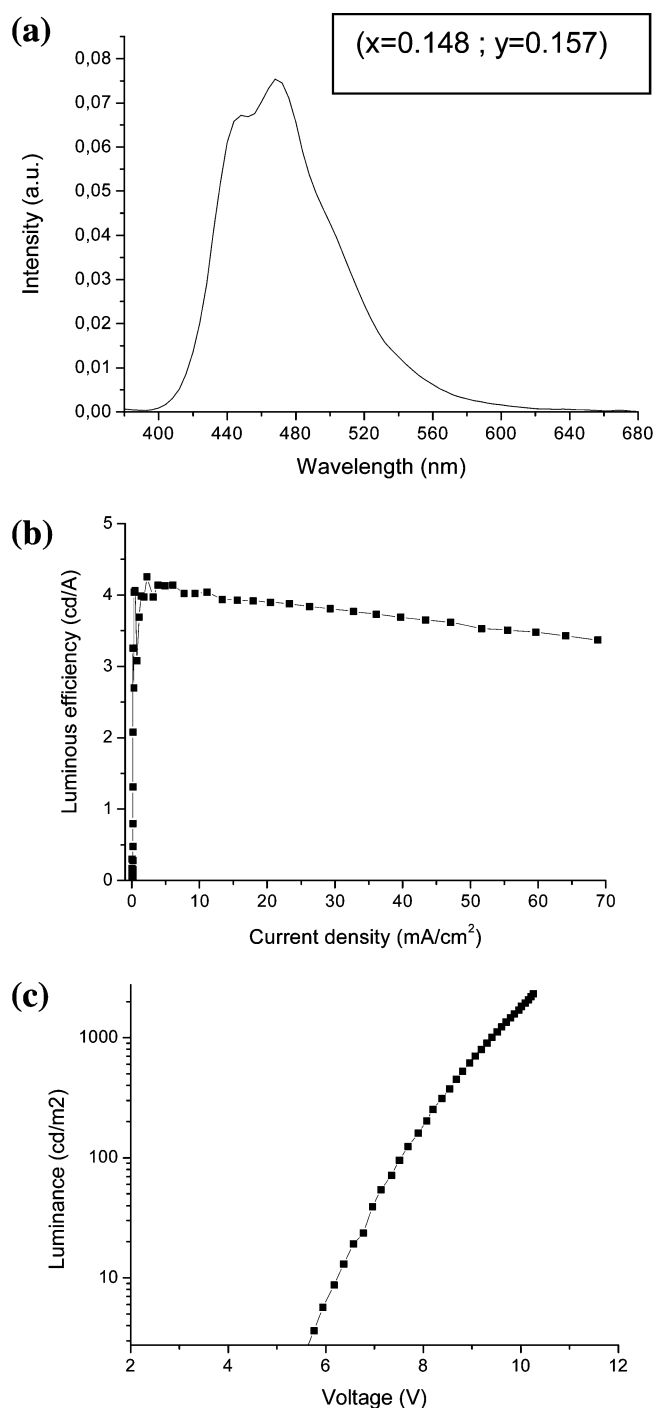


Figure 6. (a) EL spectrum and CIE coordinates at 10 mA/cm^2 , (b) luminous efficiency—current density, and (c) luminance—voltage curves for the blue OLED.

and the reverse scan peak potentials ($E_{\text{red}}^\circ = -1.83 \text{ V vs SCE}$).

In oxidation, only one irreversible process has been observed. This peak remains irreversible even when the scan rate was increased up to several hundred of volts per seconds (Figure 5b), indicating that the lifetime of the produced radical cation is shorter than 1 ms in our experimental conditions. It is noticeable that the radical-cation has a much lower chemical stability than the corresponding radical-anion. In our determination, the E_{ox}° value (Table 3) was approximated by the corresponding peak potential ($E_{\text{ox}} = 1.12 \text{ V vs SCE}$).

(27) Janietz, S.; Bradley, D. D. C.; Grell, M.; Giebeler, C.; Inbasekaran, M.; Woo, E. P. *Appl. Phys. Lett.* **1998**, *73*, 2453.

The electrochemical gap range is about 2.9 eV, E_{ox1}° being approximated by the corresponding peak potential.

As a first approximation, it was shown that for similar conjugated molecules, the reduction potential measured versus SCE electrode can be correlated to the electron affinity and thus to the LUMO energy level,²⁷ according to the following equation: $EA \approx (E_{\text{red}} + 4.75)$. A similar relationship can be made for the oxidation potential, the ionization potential, and HOMO energies ($IP \approx E_{\text{ox}} + 4.75$).²⁸ The calculation shows that **IV** possesses a relatively high electron affinity ($EA \approx 3.0$ eV), indicating that electrons could be easily injected in a layer of **IV**. This value is in the same range as those previously determined on 6,6'-distyryl-3,3'-bipyridine derivatives despite the change from a phenyl to a thiophene ring.^{12b} On the other hand, the estimated ionization potential is about 5.9 eV.

3.6. Electroluminescent Device. Among the compounds, **IV** was selected for the device fabrication because of its blue emission in solution and its better volatility. The EL device was not optimized, and preliminarily results are reported here. Figure 6a shows the EL spectrum of the device and its CIE coordinates. The maximum emission wavelength at 468 nm and the CIE coordinates evidence a pure blue emission. Moreover, the EL spectrum is superposable to the PL spectrum of **IV**, which implies an energy transfer from the host DPVBi to the dopant **IV** and an emission from this latest. This energy transfer is possible due to the energy levels of DPVBi and **IV** (LUMO/HOMO of 2.8 eV/5.9 eV,²⁹ and 3 eV/5.9 eV, respectively). The luminous efficiency—current density and luminance—voltage characteristics of the blue OLED are shown in Figure 6b and c, respectively. The main performances of the device at 10 mA/cm² are a luminous efficiency of 3.9 cd/A, a power efficiency of 1.4 lm/W, and an external quantum efficiency of 2.9%. The efficiency of this device is good regarding the pure blue CIE coordinates (0.148; 0.157) and is comparable to the bright blue emissive system reported in the literature as a distyrylarylene derivatives/DPVBi system²⁹ (external quantum yield of 2.4%) or a spirobifluorene-based pyrazoloquinoline/TPBi device³⁰ (3.6% and 4.5 cd/A at (0.14;0;17)). In conclusion, **IV** seems

to be a promising dopant, and the device structures (thickness and rate of dopant) still have to be optimized.

4. Conclusion

In summary, a series of π -conjugated symmetric and nonsymmetric 6,6'-(disubstituted)-3,3'-bipyridine based chromophores was prepared, for the first time, by convergent Suzuki homo- or cross-coupling of building blocks based on 6-(arylvinylen)-3-bromopyridine derivatives and their corresponding pyridinyl boronic esters. This versatile synthetic route allowed us to obtain in high yields unsymmetrical as well as symmetrical chromophores end-capped with reactive functionalitie(s). The main advantage of this synthetic pathway is the flexibility to combine "tailor-made" building blocks depending on the expected mesogenic, electrochemical, or optical properties of the chromophore. As examples, the push—pull compounds **I** and **II** are liquid crystals, photoluminescent, and active in NLO. The symmetrical compound **IV**, which exhibits intense fluorescence emission in the blue wavelength region, is an active laser dye and has been used as an emitter in an OLED. The efficiency of this device is good regarding the pure blue CIE coordinates (0.148; 0.157).

Thus, all of these results made this modular synthetic approach very attractive in several optoelectronic fields. As an example, the synthesis of NLO (i) organic chromophores bearing more efficient donor/acceptor pairs and (ii) organometallic chromophores is in progress to extend the series. On the other hand, chromophores **IV** and **V** will be incorporated either as lateral groups in side-chain polymers or as a repeating unit in main-chain polymers, respectively, to elaborate PLEDs and investigate the effect of the copolymer structures on the photophysical properties.

Acknowledgment. We thank Drs. Christine Denis and Pascal Maise (CEA/LITEN/GENEC/L2C) for the realization of the LED. Drs. Emmanuel Rosencher and Michel Lefebvre (ONERA - DMPH) are gratefully acknowledged for their assistance in performing laser characterizations.

Supporting Information Available: Syntheses of **3**, **5**, **Br2**, **Br5**, **B3**, and chromophores **I–V**, ¹H NMR spectra of chromophores, Figure 1S, and Table 1S. This material is available free of charge via the Internet at <http://pubs.acs.org>.

CM040358K

- (28) Brédas, J.-L.; Silbey, R.; Boudreaux, D. S.; Chance, R. R. *J. Am. Chem. Soc.* **1983**, *105*, 6555.
(29) Hosokawa, C.; Higashi, H.; Nakamura, H.; Kusumoto, T. *Appl. Phys. Lett.* **1995**, *67*, 3853.
(30) Chen, C.-H.; Wu, F.-I.; Chien, C.-H.; Tao, Y.-T. *J. Mater. Chem.* **2004**, *14*, 1585.